Supplementary Information

Title: Sub-diffraction Laser Synthesis of Silicon Nanowires

James I. Mitchell, Nan Zhou, Woongsik Nam, Luis M. Traverso, Xianfan Xu*

School of Mechanical Engineering, Birck Nanotechnology Center

Purdue University, West Lafayette, Indiana 47907

1 Zone Plate Efficiency Calculation

The diffraction efficiency of our zone plate was calculated as the ratio of the output power in the central peak of the focal spot and the total power incident on the zone plate. The total incident power was given by the product of the incident laser power intensity and the area of the zone plate. To get the output power at the focal plane, we evaluated the diffracted field distribution at the focal plane using the analytical method by Cao and Jahns[1], and integrated the diffracted power over the central peak. The efficiency of our zone plate was 15.8 percent from this calculation. This efficiency is used to compute the laser fluence at the focus spot.

2 Calculations of the Modification of the Optical Properties by Laser Pulses

To calculate the modification of the optical properties by laser pulses, we first estimated the carrier density, and modeled the propagation of the laser beam inside silicon dioxide using a (2+1)-dimensional wave propagation equation[2], and solved it simultaneously with the rate equation of the carrier density. The dielectric function of silicon dioxide is described by the Drude model, and modified by the femtosecond laser pulse considering carrier generation caused by nonlinear photoionization. At the maximum fluence of 0.029 J/cm^2 used in the experiment, the maximum subsurface carrier density is found to be 5.76×10^{19} cm^{-3}, which is substantially smaller than the critical density 1.4×10^{22} cm^{-3}, indicating a negligible modification of silicon dioxide. With the dielectric constant $\varepsilon_{SiO_2,1} = 2.152$ calculated from the estimated carrier density,

a frequency-domain FEM is employed to calculate the field distribution on the silicon dioxide surface illuminated by a femtosecond laser with a wavelength of 395 nm.

3 Intensity Distribution when Two Wires are Formed

In the experiment, two wires were also observed. It is shown in **Fig. S1** that if the laser beam is focused between the two wires, possibly due to the misalignment between the polarization direction and the moving direction of the piezoelectric stage, two high intensity spots at the wire ends are produced, resulting in the synthesis of silicon.

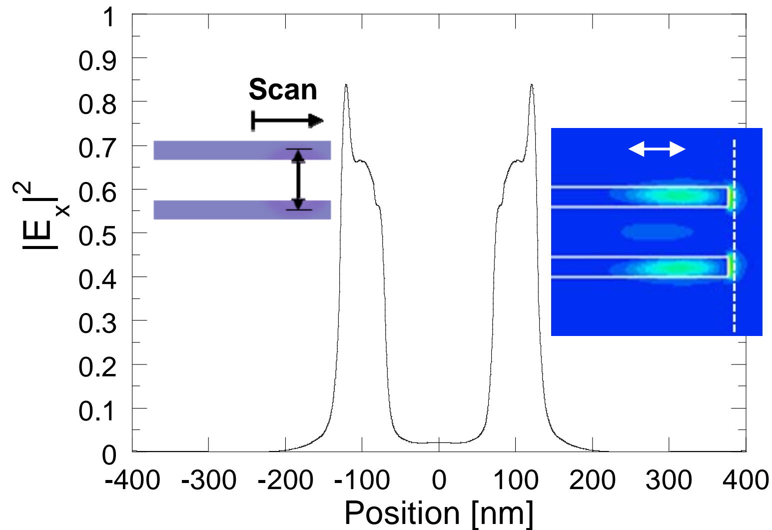

Fig. S1. $|E_x|^2$ distributions for two nanowires along the dash line in the inset. The wires are 30 nm high with a semi-circular cross section. The spacing between wires is 180 nm. The white arrow indicates the polarization of the electric field.

4 Plasmonic Effect

To further examine the interference mechanism between the incident laser beam, scattered laser radiation, and the possible surface plasmonic wave, we carried out FEM

simulations with the commercial software High Frequency Structural Simulator (HFSS) version 14 to compare both slightly-excited and highly-excited silicon dioxide surfaces with a normally incident plane wave. Using a simulated 250 nm diameter laser beam focused on the end of a silicon wire laying on a silicon dioxide substrate with the polarization of the electrical field of the laser beam parallel to the wire, the slightly-excited surface is irradiated by a laser fluence of 0.029 J/cm^2, the maximum laser fluence used in our experiments, resulting in a dielectric constant $\varepsilon_{SiO_2,1} = 2.152$, and the highly-excited surface is assumed to be irradiated by a laser fluence of 1.67 J/cm^2, resulting in a dielectric constant of $\varepsilon_{SiO_2,2} = -11.47 + i2.89$, corresponding to a carrier density of about 8.5×10^{22} cm^{-3} using the laser beam propagation calculations described above. **Figures S2A-B** show the $|E_x|^2$ distribution on the silicon dioxide surfaces normalized for an incident electric field E = 1 V/m. The orientation of fringes at the low incident laser fluence is parallel to the laser polarization as shown in **Fig. S2A**, which is consistent with what we observed in nanowire growth. For the high laser fluence, the fringes switch orientation to be perpendicular to the laser polarization direction, as shown in **Fig. S2B**, and is consistent with previous research[3,4] for laser ablation of dielectric materials. The calculated spacing of fringes as labeled in **Fig. S2B** is close to the theoretical wavelength of surface plasmon, 377 nm, using $\lambda_{SPP} = \lambda_0 \sqrt{\frac{\varepsilon_1 + \varepsilon_2}{\varepsilon_1 \varepsilon_2}}$, where $\lambda_0 = 395\, nm$, $\varepsilon_1 = \mathrm{Re}(\varepsilon_{SiO_2,2}) = -11.47$ and $\varepsilon_2 = 1$ for air.

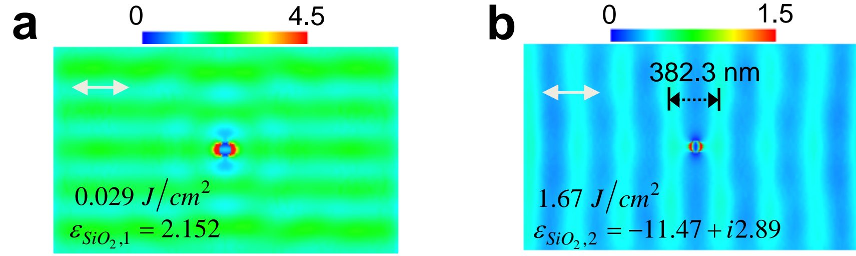

Fig. S2. $|E_x|^2$ distributions for silicon dot excitation. The distributions are for (A) slightly-excited and (B) highly-excited silicon dioxide surfaces. The fluences and corresponding dielectric constants for different surfaces are as labeled.

5 Estimation of Temperature Increase

The temperature rise during high repetition rate (>80 MHz) laser heating comes from two parts, one is the accumulative laser heating by quasi-CW behavior of the high repetition rate laser pulses, the other is the peak temperature rise from a single laser pulse. The temperature rise due to accumulative heating is calculated using the finite element package ANSYS (ANSYS Inc.). The heat source was scanned at a speed of 0.5 µm/s. The multiple layer sample was represented using a symmetric model consisting of fused quartz coated with a layer of 200 nm-thick poly-silicon and a layer of 200 nm-thick SiO_2, same as the structure used in the experiments. The entire volume was discretized into 212,104 nodes and 166,385 elements of varied sizes. Temperature dependent material properties were used [5]. Volumetric heat generation profile was applied and the values for absorption coefficient were 2594/m and 1.213 $\times 10^7$ /m for SiO_2 and silicon, respectively, the former was obtained from numerical calculations described previously for calculating the permittivity modified by a femtosecond laser pulse. The results showed the maximum accumulative temperature rise is 27.4 K for a laser fluence of 0.029

J/ cm^2. The temperature rise due to a single femtosecond laser pulse heating was found to be 467 K at 0.012 J/ cm^2 input laser fluence, and 1128 K at 0.029 J/ cm^2.

Silane decomposition starts from 380°C to 450°C [6]. From this we can conclude that the accumulative heating from high repetition pulses provides a small temperature rise while the main heating for silane decomposition and nanowire growth was provided by the peak temperature achieved during each pulse.

References:

1. Q. Cao, J. Jahns, Comprehensive focusing analysis of various Fresnel zone plates. *J. Opt. Soc. Am. A* **21**, 561-71 (2004).
2. A. Q. Wu, I. H. Chowdhury, X. Xu, Femtosecond laser absorption in fused silica: Numerical and experimental investigation. *Phys. Rev. B* **72**, 085128 (2005).
3. Huang, M., Zhao, F., Chong, Y., Xu, N. & Xu, Z. Origin of laser-induced near-subwavelength ripples: Interference between surface plasmons and incident laser. *ACS Nano* **3**, 4062-70 (2009).
4. Shimotsuma, Y., Kazansky, P. G., Qiu, J. & Hirao, K. Self-organized nanogratings in glass irradiated by ultrashort light pulses. *Phys. Rev. Lett.* **91**, 247405 (2003).
5. Incropera, F. P., Dewitt, D. P., Bergman, T. L., & Lavine, A. S., *Fundamentals of Heat and Mass Transfer.* (Wiley, Hoboken, 2005).
6. Hogness, T.R., Wilson, T.L., & Johnson, W.C. The thermal decomposition of silane. *J. Am. Chem. Soc.* **1**, 108–112 (1936).